






## Investigation of Ni- and Co-Based Bifunctional Electrocatalysts for Carbon-Free Air Electrodes Designed for Zinc-Air Batteries

Emiliya Mladenova<sup>1</sup>, Miglena Slavova<sup>1, 2\*</sup> , Borislav Abrashev<sup>1</sup> , Valentin Terziev<sup>1</sup>,  
Blagoy Burdin<sup>1</sup>, Gergana Raikova<sup>1</sup> 

<sup>1</sup> Acad. Evgeni Budevski Institute of Electrochemistry and Energy Systems, Bulgarian Academy of Sciences, Acad. G. Bonchev Str., Bl. 10, Sofia 1113, Bulgaria.

<sup>2</sup> "Todor Kableshkov" University of Transport, 158 Geo Milev Str., 1574 Sofia, Bulgaria.

### Abstract

Ni- and Co-oxide materials have promising electrocatalytic properties towards the oxygen evolution reaction (OER) and the oxygen reduction reaction (ORR), and attract with low cost, availability, and environmental friendliness. The stability of these materials in alkaline media has made them the most studied candidates for practical applications such as a gas diffusion electrode (GDE) for rechargeable metal-air batteries. In this work, we propose a novel concept for a carbon-free gas GDE design. A mixture of catalyst (Co<sub>3</sub>O<sub>4</sub>, NiCo<sub>2</sub>O<sub>4</sub>) and polytetrafluoroethylene was hot pressed onto a stainless-steel mesh as the current collector. To enhance the electrical conductivity and, thus, increase ORR performances, up to 70 wt.% Ni powder was included. The GDEs produced in this way were examined in a half-cell configuration with a 6 M KOH electrolyte, stainless steel counter electrode, and hydrogen reference electrode at room temperature. Electrochemical tests were performed and coupled with microstructural observations to evaluate the properties of the present oxygen electrodes in terms of their bifunctionality and stability enhancement. The electrochemical behavior of the new types of gas-diffusion electrodes, Ni/Co<sub>3</sub>O<sub>4</sub> and Ni/NiCo<sub>2</sub>O<sub>4</sub>, shows acceptable overpotentials for OER and ORR. Better mechanical and chemical stability of electrodes consisting of Ni/NiCo<sub>2</sub>O<sub>4</sub> (70:30 wt.%) was registered.

### Keywords:

Reversible Ni-Based Gas Diffusion Electrode;  
NiCo<sub>2</sub>O<sub>4</sub> Based Bifunctional Electrocatalyst;  
Co<sub>3</sub>O<sub>4</sub> Based Bifunctional Electrocatalyst;  
Alkaline Media;  
Carbon-Free Gas Diffusion Electrode Design.

### Article History:

|                          |    |          |      |
|--------------------------|----|----------|------|
| <b>Received:</b>         | 18 | December | 2022 |
| <b>Revised:</b>          | 08 | March    | 2023 |
| <b>Accepted:</b>         | 03 | April    | 2023 |
| <b>Available online:</b> | 14 | May      | 2023 |

## 1- Introduction

In order to turn renewable energy sources (RES) into the main energy source, it is necessary to first think about storing the excess of produced energy. The existing battery technologies require "innovative solutions, next-generation technologies, including potentially revolutionary technologies," to answer this challenge in the short term [1, 2]. Rechargeable batteries and hydrogen installations are of crucial significance and play a very important and systematic role in the integration and optimization of the consumption of RES. The expectation from battery power stations is for them to provide load shifting, peak shaving, time shifting, and frequency leveling, thus providing for intelligent grid balancing. They should be able to withstand heavy loads at charge and discharge in a time interval of a few seconds to a few hours and to be charged/discharged from one/two to dozens of cycles per day. One of the promising systems for practical application, accepted as an alternative to lithium batteries, is the zinc-air system. Using oxygen from the air, they have only one electrode, which lightens up the cell's construction. This distinguishes zinc-air batteries for both electromobility and economical storage of energy from RES due to their high theoretical energy [3–5]. The raw materials are inexpensive and non-toxic, which additionally attracts the intensive development of this kind of battery. However, the commercialization of electrically rechargeable zinc-air batteries is still limited due to the fast electrode degradation during cycling and the rapid decrease in their capacity.

\* **CONTACT:** [mslavova@iees.bas.bg](mailto:moslavova@iees.bas.bg)

**DOI:** <http://dx.doi.org/10.28991/ESJ-2023-07-03-023>

© 2023 by the authors. Licensee ESJ, Italy. This is an open access article under the terms and conditions of the Creative Commons Attribution (CC-BY) license (<https://creativecommons.org/licenses/by/4.0/>).

The main components of the Zn-air cells are similar to those used in fuel cells: a metal electrode, an alkaline electrolyte, a separator, and an air (gas diffusion) electrode (Figure 1). As the present study concerns the GDE investigation, the structure of the air electrode will be described in more detail. It consists of a gas diffusion layer (GDL), which provides the needed oxygen, and a catalytic layer (CL), where electrochemical reduction of oxygen at discharge and oxygen evolution during charging occur [6]. The following steps are involved: (i) Diffusion of oxygen to the three-phase boundary, which is the reaction zone; (ii) Adsorption of the oxygen at the three-phase boundary; (iii) Electron transfer to the adsorbed oxygen (electrochemical step); (iv) Removal of the reaction products ( $\text{OH}^-$ ,  $\text{H}_2\text{O}_2$ ,  $\text{H}_2\text{O}$ ) through the electrolyte [7].

Due to their large surface area, active carbon or carbon blacks are the most commonly used materials for GDL preparation. Polytetrafluoroethylene is applied as a hydrophobic bonding material to provide permeability for oxygen but not for the electrolyte.

Intensive investigation of many new electrocatalysts has been reported, but most of the studies involve carbon as a support and electronic conductor [8–13]. The carbon implantation, as support and/or active catalytic reactant, leads to high electrochemical carbon corrosion during the oxygen evolution reaction (OER) and reduces the electrode stability, which makes the GDE preparation crucial for the total battery performance. The production of a bifunctional oxygen electrode without carbon components is the aim of the current research.

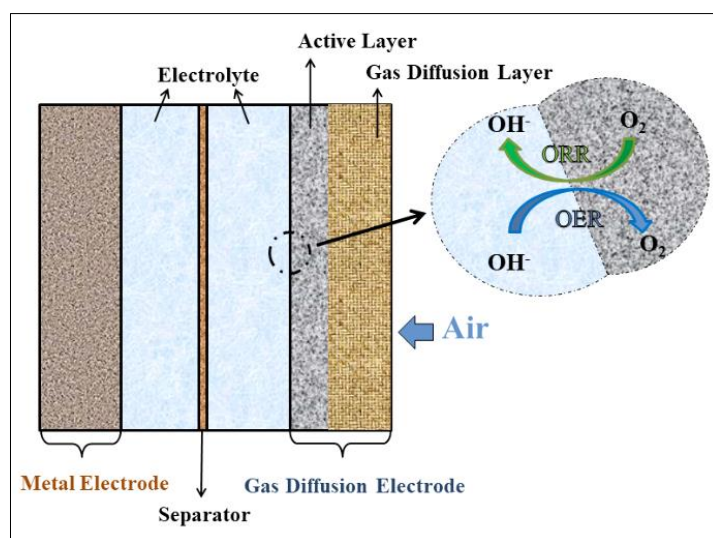


**Figure 1. Schematic illustration of rechargeable metal-air system**

Based on well-known Ni- and Co-based bifunctional electrocatalysts, we propose a novel concept for a gas diffusion electrode design fabricated by only one active material and a hydrophobic binder. Due to their high reactivity to the OER and the ORR, as well as their low cost, availability, and environmental friendliness, they have received considerable attention over the past decades. The stability of this type of oxide in alkaline media has made them the most studied candidates for practical application as a GDE, and a wide variety of methods and techniques to achieve controlled morphology of their bifunctionality have been reported [14–22].

Transition metal oxides are extensively studied for high-performance energy storage applications [23]. Some of the most promising mixtures of transition metal oxides as electrocatalysts are those with a spinel structure and atomic arrangement of the  $\text{AB}_2\text{O}_4$  type. A and B are metals with charges,  $\text{M}^{3+}$  and  $\text{M}^{2+}$ , respectively ( $\text{M} = 3\text{d}$  transition metal). Cobalt, in oxides with a spinel structure, shows very good electrocatalytic properties. The most representative is the coexistence of Co with different valences, such as in  $\text{Co}_3\text{O}_4$ . This promotes higher electron transfer during oxygen reactions [24]. Currently,  $\text{NiCo}_2\text{O}_4$  is one of the most frequently reported good electrocatalysts for oxygen reactions with such an atomic arrangement. The spinel-structured transition metal oxide  $\text{NiCo}_2\text{O}_4$  shows high electronic conductivity and theoretical catalytic activity compared to monometallic oxide catalysts, such as  $\text{Co}_3\text{O}_4$ , and can compete with electrocatalysts containing noble metals [25].  $\text{NiCo}_2\text{O}_4$  helps improve the OER and ORR of the positive electrode [26].

A bifunctional electrocatalyst, which is a mixture of  $\text{Co}_3\text{O}_4$ – $\text{NiCo}_2\text{O}_4$ , has been used in various developments. It has been successfully applied as a cathode electrocatalyst for Zn-air batteries and shows superior activity and excellent stability [27, 28]. Compared with pure  $\text{Co}_3\text{O}_4$ , the mixture of  $\text{Co}_3\text{O}_4$ – $\text{NiCo}_2\text{O}_4$  shows excellent ORR and OER performance [29]. To improve cathodic reduction and thus compensate for a lack of carbon, additional nickel powder is introduced. Due to its resistance to high voltage and conductive properties, Ni is widely used in various types of batteries, such as: NiCd, NiMH, NiZn, NiFe, lithium-ion batteries in the form of  $\text{LiNiMnCo}$  or  $\text{LiNiCoAlO}_2$ , etc. [30–33]. It is a cheap and easily accessible metal.

## 2- Experimental

### 2-1- Materials and Methods

A mixture of nickel powder (Alfa Aesar, particle size 300–700 nm),  $\text{Co}_3\text{O}_4$  (Marion Technologies, particle size 152 nm), or  $\text{NiCo}_2\text{O}_4$  (Marion Technologies, particle size 110 nm) with ratios in wt.% 70/30, respectively, and polytetrafluoroethylene emulsion (Sigma-Aldrich, 60 wt.% dispersion in water) with an amount of 10 wt.% was ball milled and then compressed with pressure of  $300 \text{ kg/cm}^2$  for 3 minutes at temperature of  $250 \text{ }^\circ\text{C}$  through a stainless-steel mesh, which serves as a current collector. The working area of the obtained GDE is  $10 \text{ cm}^2$ .

The same technology was applied for the production of the so-called Etalon Electrode (EE), consisting of CL prepared with Ag (Ferro AG),  $\text{Co}_3\text{O}_4$  (Marion Technologies), and PTFE powder (Good Fellow, particle size  $152 \mu\text{m}$ ) with a ratio of wt.% 70/30/10 and pressed onto the GDL impregnated with PTFE powder carbon blacks (Vulcan XC-72, Cabot Corp.) mixed with a stainless-steel mesh [31–40]. The total amount of the above-mentioned GDE with respect to both thickness (amount of catalytic mass mixed with PTFE) and the ratio between catalyst and binding agent (PTFE) is  $50 \text{ mg.cm}^{-2}$  GDL and  $40 \text{ mg.cm}^{-2}$  CL. Based on our analysis [41, 42], it is accepted as the best achievement of a carbon-based bifunctional gas diffusion electrode at the moment.

Figure 2 illustrates the flowchart to the article experimental procedure as presented in the research methodology.

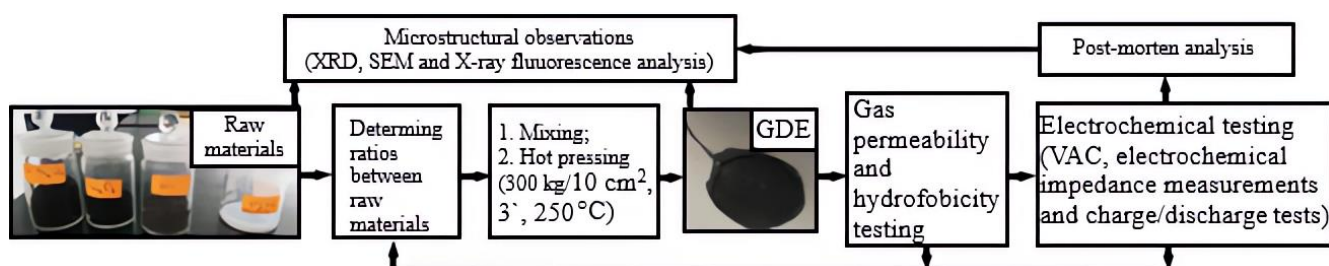


Figure 2. The experimental procedure as presented in the research methodology of the current article

### 2-2- Physicochemical Characterization

X-ray fluorescence analysis was performed on a Fischerscope XDAL apparatus (Helmut Fischer, Germany). X-ray diffraction (XRD) data were collected on an APD 15 Philips 2134 diffractometer employing  $\text{CuK}\alpha$  radiation ( $\lambda = 0.15418 \text{ nm}$ ) operated at  $U = 40 \text{ kV}$  and  $I = 30 \text{ mA}$ . The crystalline phases were identified using Joint Committee on Powder Diffraction Standards (JCPDS) files. Electron microscope JEOL 6390, with an INCA Oxford EDS detector was used for morphology observations. The entire sample was evaluated immediately after its preparation for gas permeability and hydrophobicity. The tests were performed in a home-made installation described in more detail in Mladenova et al. [43] and Slavova et al. [44].

### 2-3- Electrochemical Testing

The electrochemical measurements were done in a homemade three-electrode cell (Figure 3) in half-cell configuration at room temperature in  $6 \text{ M KOH}$  electrolyte vs. hydrogen reference electrode (RHE, Gaskatel) and stainless-steel counter electrode. Air was used as feed gas during discharge.

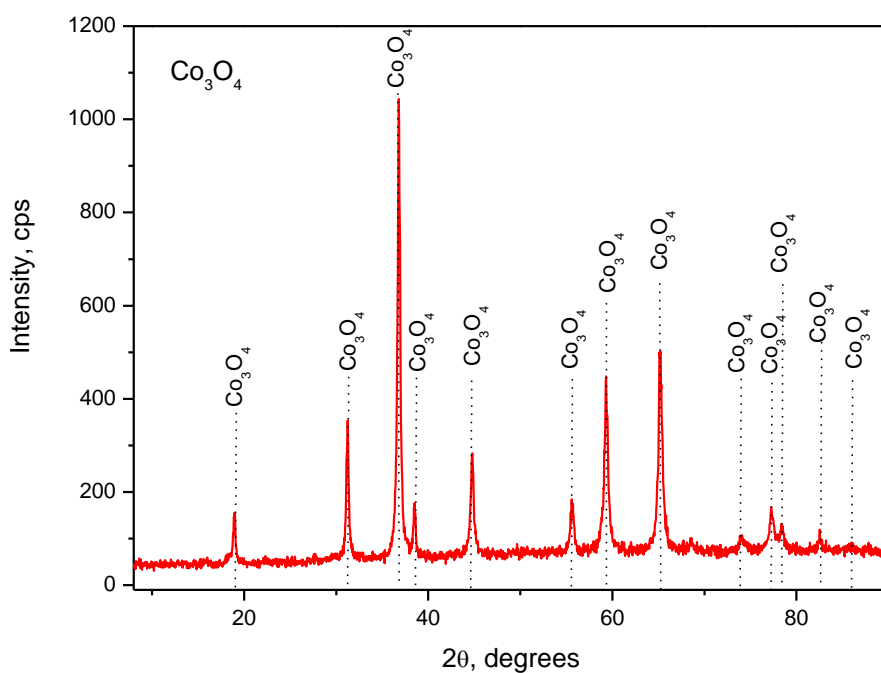


Figure 3. General view of the specially designed three-electrode unit cell

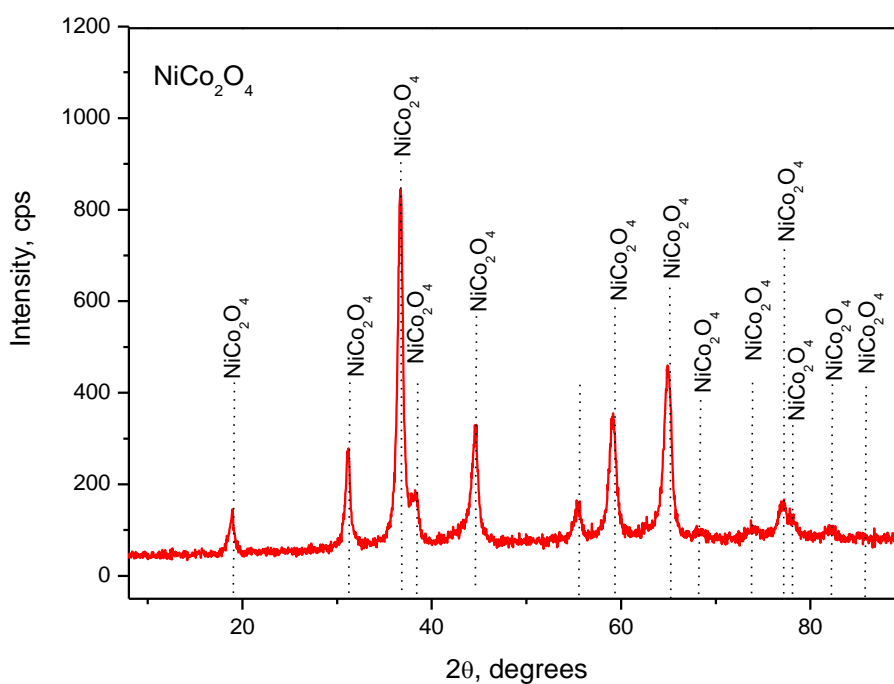
Volt-ampere characteristics (VAC) were recorded using a Solartron Schumberger 1820 potentiostat and a Tacussel (Bi-PAD) with a specialized electrochemical program, that allows for potential evaluation within a pre-defined range with a given speed and current flow registered. The electrochemical impedance measurements were performed on the IVIUM—CompactStat e10030 at a frequency range of 1 MHz–0.01 Hz, with a density of 5 points/decade and an amplitude of the AC signal of 1 mA. Charge/discharge tests were performed using an eight-channel Galvanostate 54 (PMC) working in the potential range -1.0 V to +2 V in the following usage conditions: charged (OER) for 45 min. and discharged (ORR) for 30 min. with a current density  $\pm 20 \text{ mA cm}^{-2}$ .

### 3- Results and Discussion

The XRD patterns recorded on both powders as received from the producer are presented in Figures 4a and 4b. The results, summarized in Table 1, represent a single-phase cubic crystal system with a spinel structure. SEM observation of  $\text{Co}_3\text{O}_4$  catalysts (Figure 4c) shows similar-sized spherical particles distributed uniformly, whereas significantly smaller particles on the  $\text{NiCo}_2\text{O}_4$  surface are observed (Figure 4d), which is in agreement with the X-ray phase analysis data.



(a)



(b)



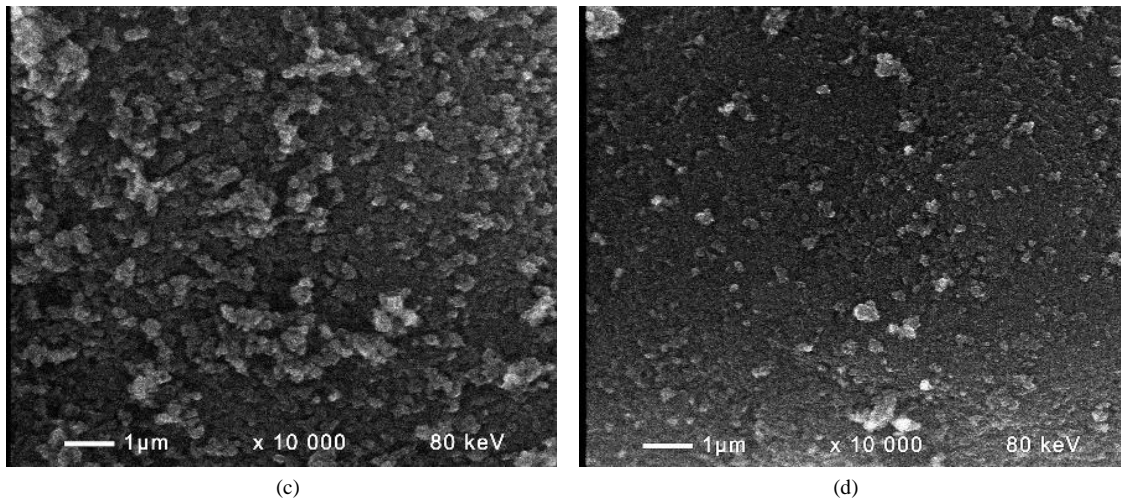
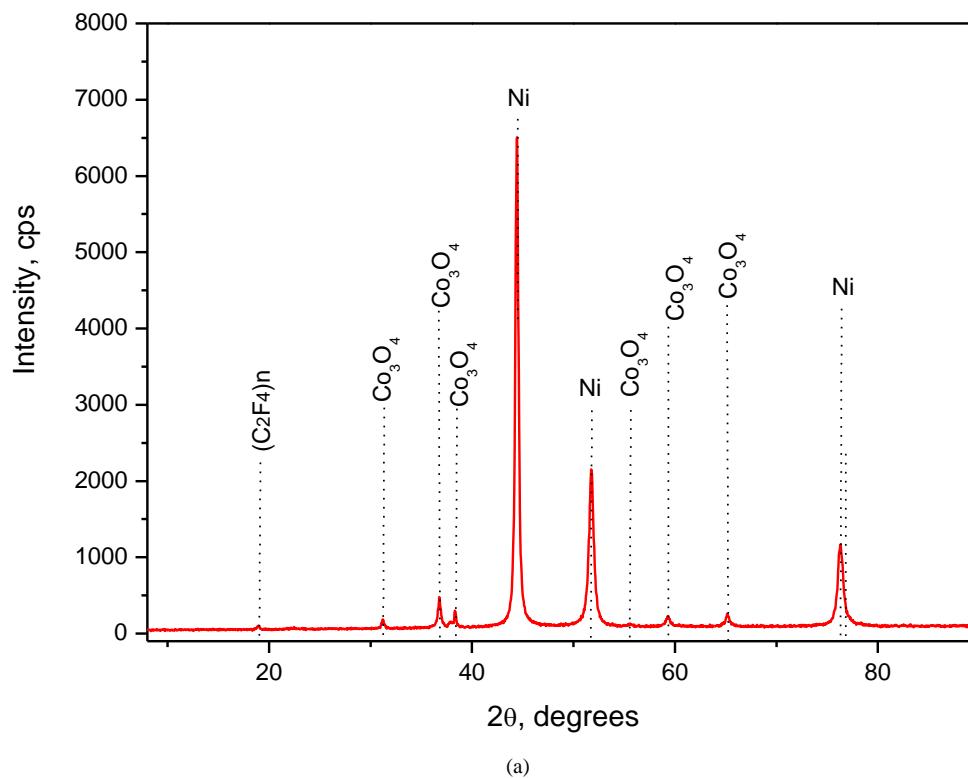


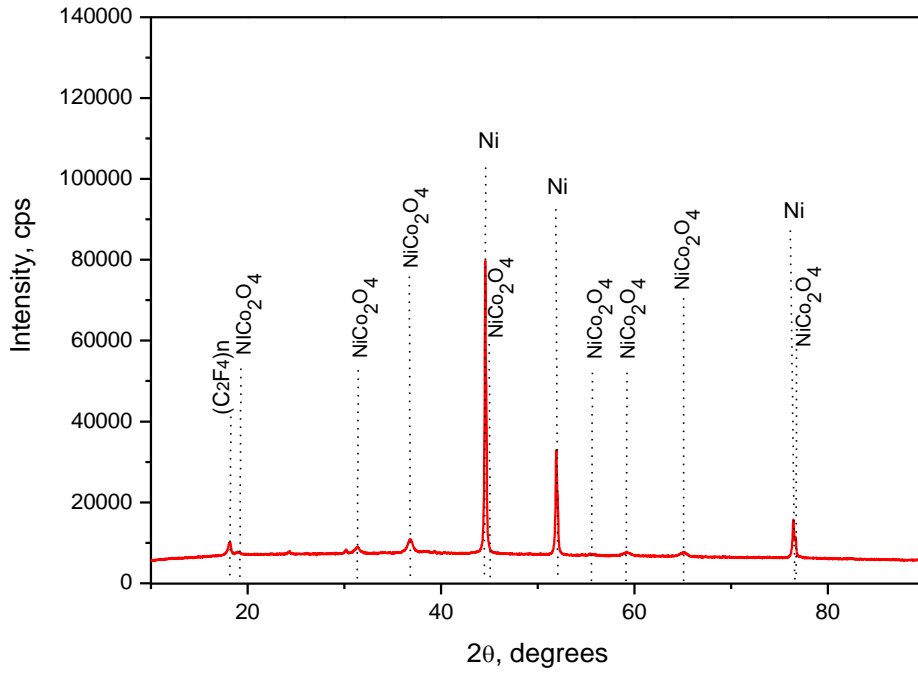
**Figure 4.** XRD patterns of  $\text{Co}_3\text{O}_4$  (a) and  $\text{NiCo}_2\text{O}_4$  (b) catalysts and SEM images of raw  $\text{Co}_3\text{O}_4$  (c) and  $\text{NiCo}_2\text{O}_4$  (d) spinel

**Table 1.** Crystallographic parameters of  $\text{Co}_3\text{O}_4$  and  $\text{NiCo}_2\text{O}_4$  powders

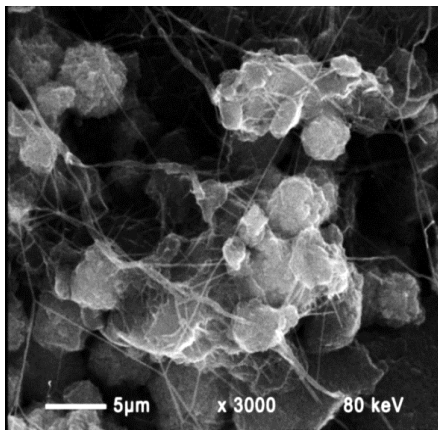
| Phase                     | $a$ (Å) | $2\theta$ (degree) | $L$ (nm) | vol. % | Intensity (%) | ICCD        |
|---------------------------|---------|--------------------|----------|--------|---------------|-------------|
| $\text{Co}_3\text{O}_4$   | 8.0837  | 36.853             | 33.6     | 100    | 100.0         | 00-042-1467 |
| $\text{NiCo}_2\text{O}_4$ | 8.1100  | 36.697             | 15.6     | 100    | 100.0         | 00-020-0781 |
| Ni-standard               | 3.5238  | -                  | -        | -      | -             | 00-004-0850 |

Microstructural observations on the prepared electrodes are presented in Figures 5 and 6. After the addition of this high amount of nickel (70 wt.% metallic Ni), the X-Ray diffraction cannot differentiate the spinel spectra. Only peaks corresponding to the Ni phase are presented (Figures 5a and 5b). The same could be concluded from the observed X-ray fluorescence analysis (Figure 6), which results in a markedly greater amount of Ni - approximately 85 wt.% compared to 70 wt.% uploaded for the production of both electrodes,  $\text{Co}_3\text{O}_4$ - and  $\text{NiCo}_2\text{O}_4$ -based. Obviously, Ni particles, which are larger than those of spinel particles, covered  $\text{Co}_3\text{O}_4$  and  $\text{NiCo}_2\text{O}_4$  during mechanical mixing of the powders, followed by thermal treatment and pressing.

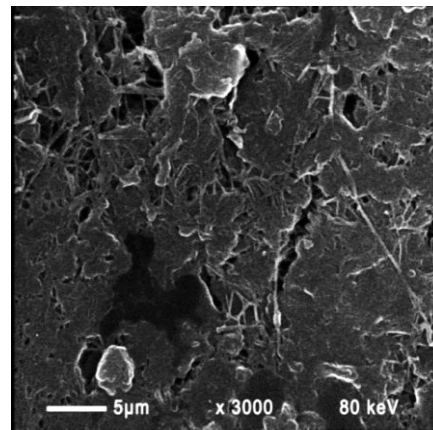




(b)

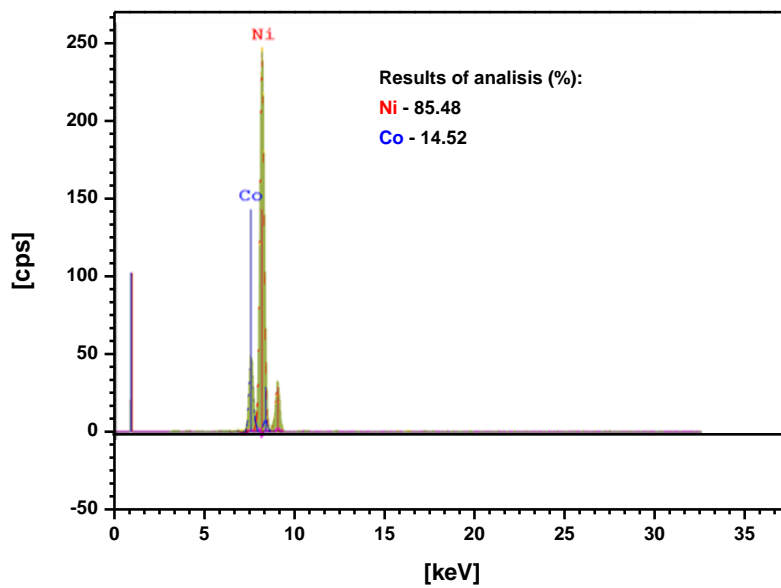


(c)

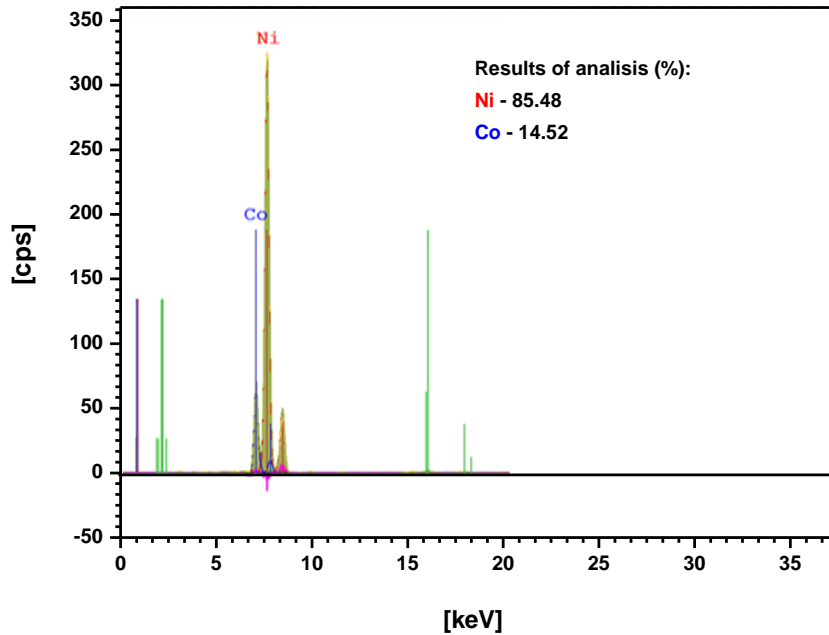


(d)

**Figure 5.** XRD patterns of pristine gas-diffusion electrodes Ni/Co<sub>3</sub>O<sub>4</sub> (a) and Ni/NiCo<sub>2</sub>O<sub>4</sub> (b) and corresponding SEM images Ni/Co<sub>3</sub>O<sub>4</sub> (c) and Ni/NiCo<sub>2</sub>O<sub>4</sub> (d)



(a)



(b)

**Figure 6.** X-ray fluorescence analysis of pristine gas-diffusion electrodes Ni/Co<sub>3</sub>O<sub>4</sub> (a) and Ni/NiCo<sub>2</sub>O<sub>4</sub> (b)

The performance of the electrodes was further evaluated by electrochemical tests. Figure 7 shows the VAC characteristics of the investigated GDEs, and a comparison with the Etalon Electrode (EE) is done. The behavior of the electrodes is similar to that of EE. It can be seen that the Ni/NiCo<sub>2</sub>O<sub>4</sub> electrode performed slightly better than EE, but the difference in performance decreased with increasing the current density. During reduction, it reached a current density of 40 mA/cm<sup>2</sup>, while the Ni/Co<sub>3</sub>O<sub>4</sub> electrode reached only half of this value (20 mA/cm<sup>2</sup>).

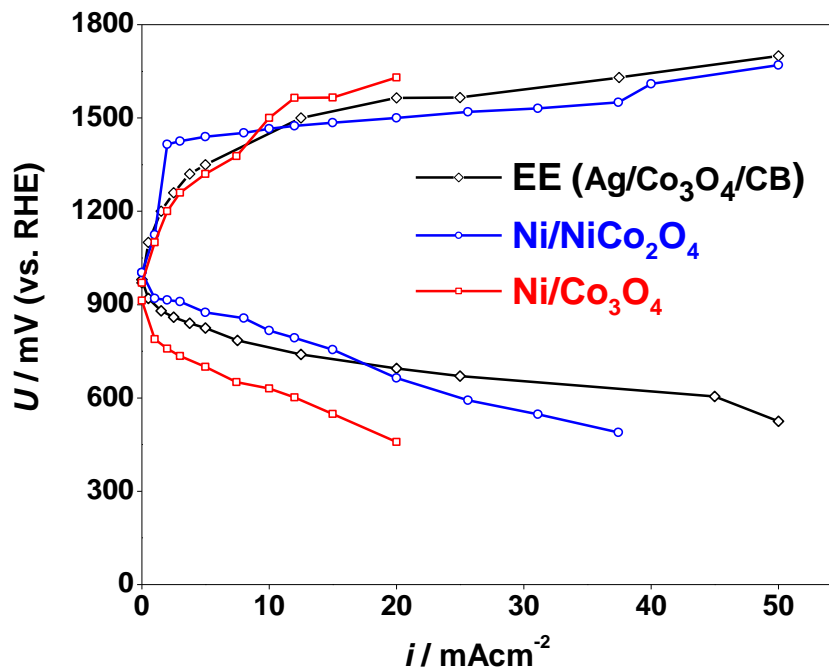


**Figure 7.** Volt-ampere characteristics of Ni/Co<sub>3</sub>O<sub>4</sub> (□) and Ni/NiCo<sub>2</sub>O<sub>4</sub> (○) electrodes during charge (OER) and discharge (ORR). A comparison with the Etalon Electrode (EE) is given (◇)

Impedance measurements were performed periodically during the discharge (ORR) tests, aiming to cover the electrode behavior during the three characteristic slopes of the I/V curves with the following operating points selected: 5 mA, 10 mA, and 20 mA. The obtained impedance spectra were analyzed using the equivalent circuit presented in Figure 8. The results are summarized in Table 2, and some Nyquist plots are presented in Figure 9.

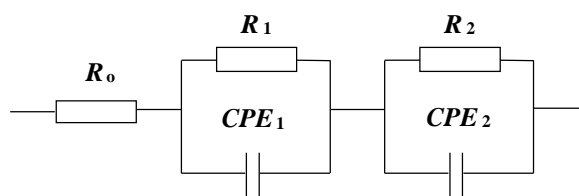
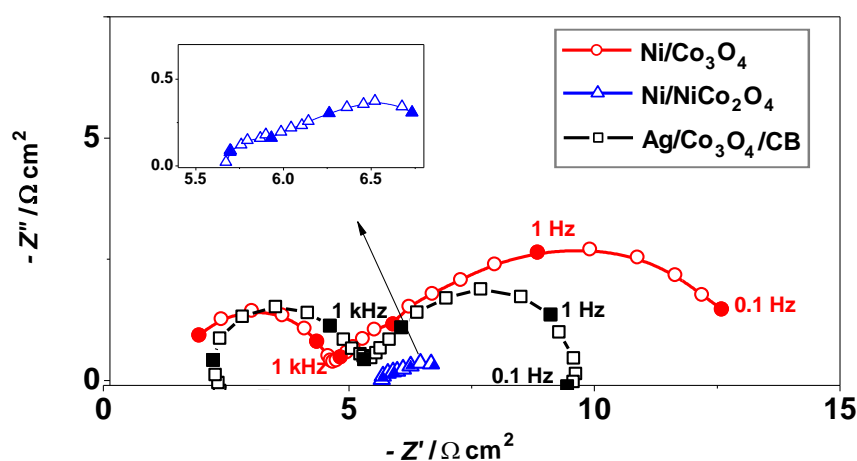


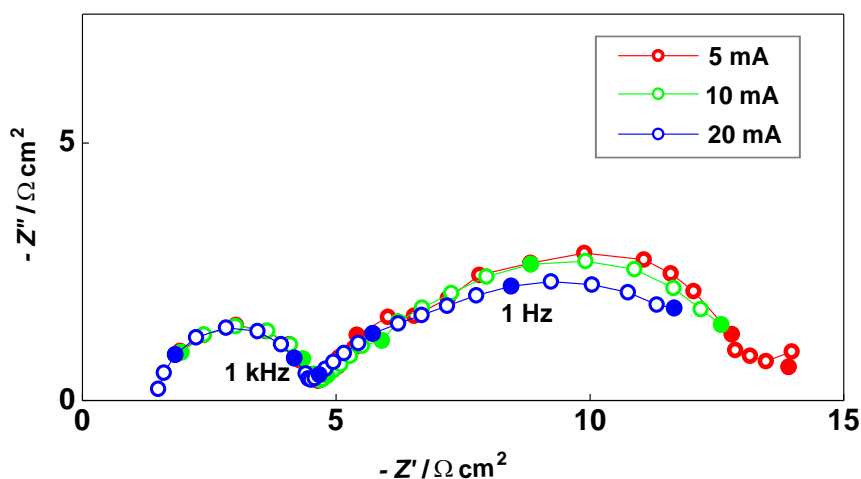
Figure 8. Equivalent circuit

Table 2. Values of polarization and total resistance in three working point during ORR of carbon-free GDEs

| Electrode                             | Working point | $R_o / \Omega cm^2$ | $R_1 / \Omega cm^2$ | $R_2 / \Omega cm^2$ | $R_p / \Omega cm^2$ |
|---------------------------------------|---------------|---------------------|---------------------|---------------------|---------------------|
| Ni/Co <sub>3</sub> O <sub>4</sub>     | 5mA           | 1.52                | 4.64                | 14.26               | 12.74               |
|                                       | 10mA          | 1.51                | 4.71                | 14.32               | 12.81               |
|                                       | 20mA          | 1.51                | 4.52                | 14.62               | 13.11               |
| Ni/NiCo <sub>2</sub> O <sub>4</sub>   | 5mA           | 3.10                | 4.45                | 6.13                | 3.03                |
|                                       | 10mA          | 5.26                | 6.12                | 7.23                | 1.97                |
|                                       | 20mA          | 5.68                | 6.05                | 7.54                | 1.86                |
| Ag/Co <sub>3</sub> O <sub>4</sub> /CB | 10mA          | 1.95                | 5.32                | 9.73                | 12.74               |



(a)



(b)

Figure 9. Impedance data of EE, Ag/ Co<sub>3</sub>O<sub>4</sub>/CB (□); Ni/Co<sub>3</sub>O<sub>4</sub> (○) Ni/NiCo<sub>2</sub>O<sub>3</sub> and Ni/NiCo<sub>2</sub>O<sub>4</sub> (Δ) GDEs measured at working point  $i=10mA$  during ORR (a) and the influence of the cathodic current densities on the Ni/Co<sub>3</sub>O<sub>4</sub> electrode resistance (b).

The internal resistance ( $R_o$ ) and the charge-transfer resistance ( $R_1$ ) of the Ni/Co<sub>3</sub>O<sub>4</sub> electrode are approximately the same as those of the Etalon, since significant differences in low frequency semicircles are observed ( $R_2$ ). They are



dominated by the diffusion process and can be attributed to the different microstructures. The porous and highly active carbon surface area contributes to the fast transport of oxygen from the atmospheric air to the catalytic zones, i.e., the three-phase boundary where the electrochemical reduction takes place. On the contrary, the higher initial resistance obtained for the Ni/NiCo<sub>2</sub>O<sub>3</sub> electrode demonstrates that some activation processes occurred at the electrode surface. However, this electrode exhibited better performance in oxygen reduction, displaying a lower charge-transfer resistance than that of the other two electrodes. It can be attributed to the higher electrical conductivity caused by the higher amount of Ni and the larger density and homogeneity of the electrode, which is in agreement with the microstructural observation.

Similarly to the Ni/Co<sub>3</sub>O<sub>4</sub> electrode, a transport limitation (the second semicircle on the zoomed part of Figure 9a) was observed. Its influence on cathodic current densities is presented in Figure 8b. The increase in current load affected transport processes and complicated the diffusion of oxygen, thus limiting the polarization behavior of the electrodes. The increased depression (*CPE2*) of the low frequency semicircle (Figure 9b) going to bounded conditions [45] indicates that the gas-diffusion side of the electrodes was already wetted or closed.

Long-term charge/discharge tests of the Ni/NiCo<sub>2</sub>O<sub>4</sub> electrode are presented in Figure 10. With the increase in the number of charge/discharge cycles, the cell voltage stayed stable for more than 400 cycles. A very smooth increase in the polarization was observed at about 100–150 mV. A very high cycle stability of the electrode was achieved. After 400 cycles, an accelerated degradation of the electrode was registered due to electrolyte leakage. After 430 cycles, electrode wetting was observed, which hindered the oxygen's access. A post-mortem analysis of the Ni/NiCo<sub>2</sub>O<sub>4</sub> electrode after 430 charge/discharge cycles was done (Figure 11).

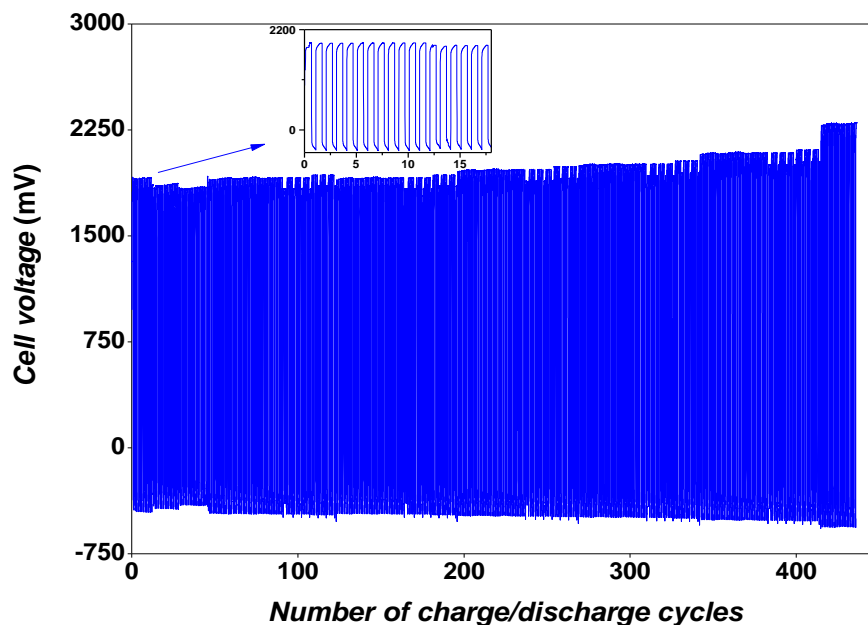
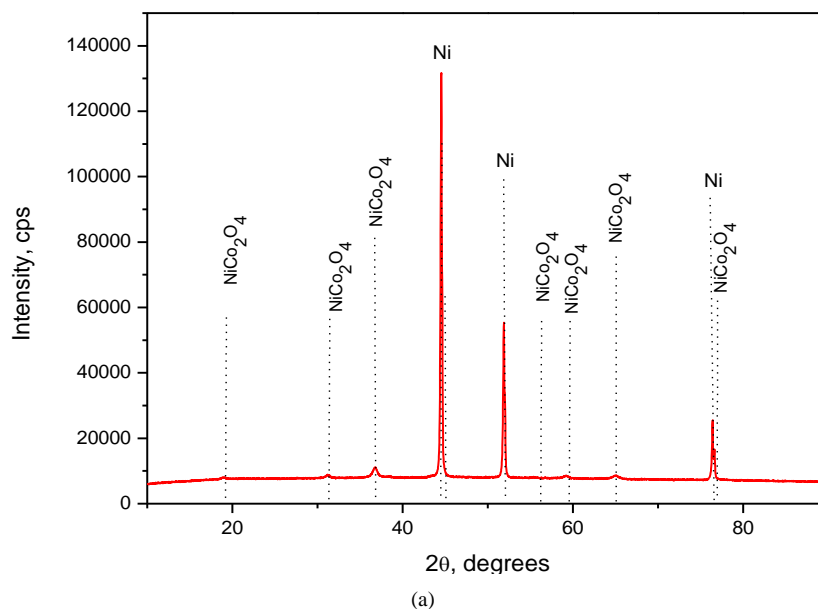
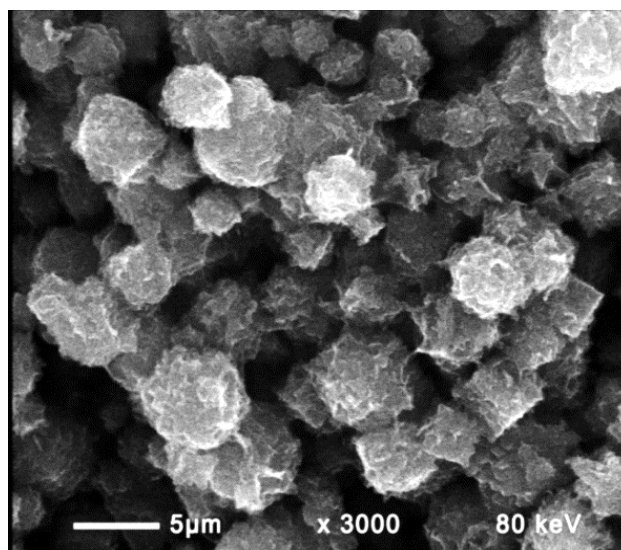


Figure 10. Charge/discharge cycling of Ni/NiCo<sub>2</sub>O<sub>4</sub> GDE





(b)

**Figure 11.** Post-mortem analysis of Ni/NiCo<sub>2</sub>O<sub>4</sub> GDE after 430 charge/discharge cycles: a) XRD pattern and b) SEM picture

The XRD and SEM observations revealed an increase in the Ni peak intensity (Figure 11-a) in comparison to those before use (Figure 4-b), due to the Ni agglomeration confirmed on the SEM picture (Figure 11-b). The PTFE streaks were no longer present, and their disbanding, caused by wetting of the electrode, caused serious damage to its functionality. NiO peaks were not present at the XDR pattern, which shows that the electrode is chemically stable and Ni corrosion processes did not occur during its operation in alkaline media.

#### 4- Conclusions

The activity and stability of spinel oxides (Co<sub>3</sub>O<sub>4</sub> and NiCo<sub>2</sub>O<sub>4</sub>) were investigated for application in a carbon-free design of reversible gas diffusion electrodes. Hot pressed mixture of these catalysts, Ni powder, and PTFE, was examined in a half-cell configuration in alkaline media. The bifunctional behavior of both electrodes (Ni/Co<sub>3</sub>O<sub>4</sub> and Ni/NiCo<sub>2</sub>O<sub>4</sub>) towards the OER and the ORR had shown acceptable overpotentials with respect to the Etalon Electrode consisting of carbon blacks. The presented monolithic electrode consists only of CL, i.e., the entire electrode is catalytically active and its electrochemical characteristics are not impaired by deeper wetting. This eliminates the possibility of poor adhesion between CL and GDL, as observed in classical GDE [46].

The impedance measurements performed during the reduction provide information about the mechanisms of the reaction. The direct 4e<sup>-</sup> reduction pathway is confirmed, which is important for energy storage applications. The diffusion of oxygen towards the three-phase boundary is recognized as the step of the reduction reaction that limits its rate. More stable electrochemical performance was registered for Ni/NiCo<sub>2</sub>O<sub>4</sub> electrodes, withstanding over 420 charge/discharge cycles. The formation of Ni agglomeration is the cause of microstructural damage to the electrode and limits its lifetime.

The proposed combination of an easy preparation procedure with non-expensive and non-toxic raw materials without carbon is very encouraging for the manufacturing of Co<sub>3</sub>O<sub>4</sub> and NiCo<sub>2</sub>O<sub>4</sub> spinel oxides based on reversible gas diffusion electrodes. The ORR activity and cycling stability can be additionally improved by decreasing the metal Ni component and by varying the catalyst/PTFE ratio to find an appropriate microstructure and increase the active surface area, thus improving the gas permeability and eliminating the Ni aggregation.

#### 5- Declarations

##### 5-1-Author Contributions

Conceptualization, E.M., M.S., and B.A.; methodology, E.M., M.S., and B.A.; validation, E.M., M.S., and B.A.; formal analysis, B.A. and V.T.; investigation, E.M., M.S., and B.A.; resources, M.S. and B.B.; data curation, B.A. and V.T.; writing—original draft preparation, E.M. and M.S.; writing—review and editing, M.S. and G.R.; visualization, M.S.; project administration, G.R.; funding acquisition, B.A. All authors have read and agreed to the published version of the manuscript.

##### 5-2-Data Availability Statement

The data presented in this study are available in the article.

### 5-3- Funding and Acknowledgements

The authors kindly acknowledge the financial support of project No BG05M2OP001-1.002-0014, Center of Competence HITMOBIL - Technologies and Systems for Generation, Storage and Consumption of Clean Energy”, funded by Operational Programme “Science and Education for Smart Growth” 2014-2020, co-funded by the EU from European Regional Development Fund and Bulgarian National Science Found Project: Innovative Rechargeable Carbon-free Zinc-Air Cells (INOVI) under GA KP-06-N27-15/14.12.2018. The equipment used is provided with the assistance of the Bulgarian Ministry of Education and Science under the National Roadmap for Research Infrastructure 2017-2023 - Energy storage and hydrogen energetics (ESHER) approved by DCM No354/29.08.2017. The authors express thanks also to the Prof. Daria Vladikova.

### 5-4- Institutional Review Board Statement

Not applicable.

### 5-5- Informed Consent Statement

Not applicable.

### 5-6- Conflicts of Interest

The authors declare that there is no conflict of interest regarding the publication of this manuscript. In addition, the ethical issues, including plagiarism, informed consent, misconduct, data fabrication and/or falsification, double publication and/or submission, and redundancies have been completely observed by the authors.

## 6- References

- [1] European Commission. (2016). Clean Energy for All Europeans. COM (2016) 860 final. European Commission, Brussels, Belgium. Available online: [https://eur-lex.europa.eu/resource.html?uri=cellar:fa6ea15b-b7b0-11e6-9e3c-01aa75ed71a1.0001.02/DOC\\_1&format=PDF](https://eur-lex.europa.eu/resource.html?uri=cellar:fa6ea15b-b7b0-11e6-9e3c-01aa75ed71a1.0001.02/DOC_1&format=PDF) (accessed on April 2023).
- [2] European Commission. (2016). Accelerating Clean Energy Innovation (COM (2016) 763 final. European Commission, Brussels, Belgium. Available online: <https://eur-lex.europa.eu/legal-content/EN/TXT/HTML/?uri=CELEX:52016DC0763&rid=4> (accessed on April 2023).
- [3] Lee, J. S., Kim, S. T., Cao, R., Choi, N. S., Liu, M., Lee, K. T., & Cho, J. (2011). Metal-air batteries with high energy density: Li-air versus Zn-air. *Advanced Energy Materials*, 1(1), 34–50. doi:10.1002/aenm.201000010.
- [4] Laabid, A., Saad, A., & Mazouz, M. (2022). Integration of Renewable Energies in Mobile Employment Promotion Units for Rural Populations. *Civil Engineering Journal*, 8(7), 1406-1434. doi:10.28991/CEJ-2022-08-07-07.
- [5] Zhang, X. G. (2006). Fibrous zinc anodes for high power batteries. *Journal of Power Sources*, 163(1), 591–597. doi:10.1016/j.jpowsour.2006.09.034.
- [6] Danner, T., Eswara, S., Schulz, V. P., & Latz, A. (2016). Characterization of gas diffusion electrodes for metal-air batteries. *Journal of Power Sources*, 324, 646–656. doi:10.1016/j.jpowsour.2016.05.108.
- [7] Haas, O., Holzer, F., Müller, K., & Müller, S. (2010). Metal/air batteries: the zinc/air case. *Handbook of Fuel Cells*, John Wiley & Sons, Hoboken, United States. doi:10.1002/9780470974001.f104022.
- [8] Velraj, S., Zhu, J., Salazar-Gastelum, M. I., Corona Sandoval, E., Beltrán-Gastélum, M., Pérez-Sicairos, S., & Félix-Navarro, R. M. (2017). Electrochemical Evaluation of LaNiO<sub>3</sub>-Based Perovskites as Bifunctional Cathode Material for Rechargeable Metal-Air Batteries. *ECS Meeting Abstracts*, MA2017-01(1), 54–54. doi:10.1149/ma2017-01/1/54.
- [9] Kar, M., Winther-Jensen, B., Forsyth, M., & MacFarlane, D. R. (2013). Chelating ionic liquids for reversible zinc electrochemistry. *Physical Chemistry Chemical Physics*, 15(19), 7191–7197. doi:10.1039/c3cp51102b.
- [10] Müller, S., Holzer, F., & Haas, O. (1998). Optimized zinc electrode for the rechargeable zinc-air battery. *Journal of Applied Electrochemistry*, 28(9), 895–898. doi:10.1023/A:1003464011815.
- [11] Haas, O., & Van Wesemael, J. (2009). Secondary Batteries - Metal-Air Systems | Zinc-Air: Electrical Recharge. *Encyclopedia of Electrochemical Power Sources*, 384–392, Elsevier Science Ltd, Amsterdam, Netherlands. doi:10.1016/B978-044452745-5.00169-6.
- [12] Dunn, B., Kamath, H., & Tarascon, J. M. (2011). Electrical energy storage for the grid: A battery of choices. *Science*, 334(6058), 928–935. doi:10.1126/science.1212741.
- [13] Caramia, V., & Bozzini, B. (2014). Materials science aspects of zinc-air batteries: A review. *Materials for Renewable and Sustainable Energy*, 3(2), 28. doi:10.1007/s40243-014-0028-3.
- [14] Manoharan, R., & Shukla, A. K. (1985). Oxides supported carbon air-electrodes for alkaline solution power devices. *Electrochimica Acta*, 30(2), 205–209. doi:10.1016/0013-4686(85)80083-9.

- [15] Kannan, A. M., Shukla, A. K., & Sathyanarayana, S. (1989). Oxide-based bifunctional oxygen electrode for rechargeable metal/air batteries. *Journal of Power Sources*, 25(2), 141–150. doi:10.1016/0378-7753(89)85006-2.
- [16] Heller-Ling, N., Prestat, M., Gautier, J. L., Koenig, J. F., Poillierat, G., & Chartier, P. (1997). Oxygen electroreduction mechanism at thin  $Ni_xCo_{3-x}O_4$  spinel films in a double channel electrode flow cell (DCEFC). *Electrochimica Acta*, 42(2), 197–202. doi:10.1016/0013-4686(96)00144-2.
- [17] Davari, E., & Ivey, D. G. (2018). Bifunctional electrocatalysts for Zn-air batteries. *Sustainable Energy and Fuels*, 2(1), 39–67. doi:10.1039/c7se00413c.
- [18] Yuan, X. Z., Qu, W., Zhang, X., Yao, P., & Fahlman, J. (2013). Spinel  $Ni_xCo_{2-x}O_4$  as a Bifunctional Air Electrode for Zinc Air Batteries. *ECS Transactions*, 45(29), 105–112. doi:10.1149/04529.0105ecst.
- [19] Price, S. W. T., Thompson, S. J., Li, X., Gorman, S. F., Pletcher, D., Russell, A. E., Walsh, F. C., & Wills, R. G. A. (2014). The fabrication of a bifunctional oxygen electrode without carbon components for alkaline secondary batteries. *Journal of Power Sources*, 259, 43–49. doi:10.1016/j.jpowsour.2014.02.058.
- [20] Sönmez, T., Thompson, S. J., Price, S. W. T., Pletcher, D., & Russell, A. E. (2016). Voltammetric Studies of the Mechanism of the Oxygen Reduction in Alkaline Media at the Spinel  $Co_3O_4$  and  $NiCo_2O_4$ . *Journal of The Electrochemical Society*, 163(10), H884–H890. doi:10.1149/2.0111610jes.
- [21] Osgood, H., Devaguptapu, S. V., Xu, H., Cho, J., & Wu, G. (2016). Transition metal (Fe, Co, Ni, and Mn) oxides for oxygen reduction and evolution bifunctional catalysts in alkaline media. *Nano Today*, 11(5), 601–625. doi:10.1016/j.nantod.2016.09.001.
- [22] Peng, X., Jin, X., Gao, B., Liu, Z., & Chu, P. K. (2021). Strategies to improve cobalt-based electrocatalysts for electrochemical water splitting. *Journal of Catalysis*, 398, 54–66. doi:10.1016/j.jcat.2021.04.003.
- [23] Rashti, A., Lu, X., Dobson, A., Hassani, E., Feyzbar-Khalkhali-Nejad, F., He, K., & Oh, T. S. (2021). Tuning MOF-Derived  $Co_3O_4/NiCo_2O_4$  Nanostructures for High-Performance Energy Storage. *ACS Applied Energy Materials*, 4(2), 1537–1547. doi:10.1021/acs.aem.0c02736.
- [24] Béjar, J., Espinosa-Magaña, F., Guerra-Balcázar, M., Ledesma-García, J., Álvarez-Contreras, L., Arjona, N., & Arriaga, L. G. (2020). Three-Dimensional-Order Macroporous  $AB_2O_4$  Spinel (A, B = Co and Mn) as Electrodes in Zn-Air Batteries. *ACS Applied Materials and Interfaces*, 12(48), 53760–53773. doi:10.1021/acsami.0c14920.
- [25] Yu, N.-F., Huang, W., Bao, K.-L., Chen, H., Hu, K., Zhang, Y., Huang, Q.-H., Zhu, Y., & Wu, Y.-P. (2021).  $Co_3O_4@NiCo_2O_4$  double-shelled nanocages with hierarchical hollow structure and oxygen vacancies as efficient bifunctional electrocatalysts for rechargeable Zn-air batteries. *Dalton Transactions*, 50(6), 2093–2101. doi:10.1039/d0dt03971c.
- [26] Mohamed, Z., Zhang, G., He, B., & Fan, Y. (2022). Heterostructure Necklace-like  $NiO-NiCo_2O_4$  Hybrid with Superior Catalytic Capability as Electrocatalyst for Li-Oxygen Batteries. *Engineered Science*, 17, 231–241. doi:10.30919/es8d595.
- [27] Liu, J., Meng, Y., Yu, D., Guo, C., Liu, L., & Liu, X. (2022). Synthesis of  $Co_3O_4/NiCo_2O_4$  Double-Shelled Nanocages with Enhanced Capacitive and Oxygen Evolution Reaction Properties in Battery-Supercapacitor Hybrid Devices. *SSRN Electronic Journal*. doi:10.2139/ssrn.4265572.
- [28] Zhu, Z., Zhang, J., Peng, X., Liu, Y., Cen, T., Ye, Z., & Yuan, D. (2021).  $Co_3O_4-NiCo_2O_4$  Hybrid Nanoparticles Anchored on N-Doped Reduced Graphene Oxide Nanosheets as an Efficient Catalyst for Zn-Air Batteries. *Energy and Fuels*, 35(5), 4550–4558. doi:10.1021/acs.energyfuels.0c04079.
- [29] Zhao, Y., Ding, L., Wang, X., Yang, X., He, J., Yang, B., Wang, B., Zhang, D., & Li, Z. (2021). Yolk-shell ZIF-8@ZIF-67 derived  $Co_3O_4@NiCo_2O_4$  catalysts with effective electrochemical properties for Li-O<sub>2</sub> batteries. *Journal of Alloys and Compounds*, 861, 157945. doi:10.1016/j.jallcom.2020.157945.
- [30] Geng, M., & Northwood, D. O. (2003). Development of advanced rechargeable Ni/MH and Ni/Zn batteries. *International Journal of Hydrogen Energy*, 28(6), 633–636. doi:10.1016/S0360-3199(02)00137-4.
- [31] Xu, J., Lin, F., Doeff, M. M., & Tong, W. (2017). A review of Ni-based layered oxides for rechargeable Li-ion batteries. *Journal of Materials Chemistry A*, 5(3), 874–901. doi:10.1039/C6TA07991A.
- [32] Yang, J., Chen, J., Wang, Z., Wang, Z., Zhang, Q., He, B., Zhang, T., Gong, W., Chen, M., Qi, M., Coquet, P., Shum, P., & Wei, L. (2021). High-Capacity Iron-Based Anodes for Aqueous Secondary Nickel-Iron Batteries: Recent Progress and Prospects. *ChemElectroChem*, 8(2), 274–290. doi:10.1002/celec.202001251.
- [33] Choi, J. U., Voronina, N., Sun, Y. K., & Myung, S. T. (2020). Recent Progress and Perspective of Advanced High-Energy Co-Less Ni-Rich Cathodes for Li-Ion Batteries: Yesterday, Today, and Tomorrow. *Advanced Energy Materials*, 10(42), 2002027. doi:10.1002/aenm.202002027.
- [34] Budevski, E. B., Iliev, I. D., Kaisheva, A. R., Gamburtzev, S. S., & Vakanova, E. B. (1977). Method for producing powdered wetproofed material useful in making gas-diffusion electrodes. U.S. Patent No. 4,031,033. Patent and Trademark Office, Washington, United States.

- [35] Gamburzev, S., Petrov, K., & Appleby, A. J. (2002). Silver-carbon electrocatalyst for air cathodes in alkaline fuel cells. *Journal of Applied Electrochemistry*, 32(7), 805–809. doi:10.1023/A:1020122004048.
- [36] Nikolova, V., Iliev, P., Petrov, K., Vitanov, T., Zhecheva, E., Stoyanova, R., Valov, I., & Stoychev, D. (2008). Electrocatalysts for bifunctional oxygen/air electrodes. *Journal of Power Sources*, 185(2), 727–733. doi:10.1016/j.jpowsour.2008.08.031.
- [37] Abrashev, B., Uzun, D., Hristov, H., Nicheva, D., & Petrov, K. (2016). Design of an electrochemical cell for Bi-functional Oxygen Electrode (BOE) studies. *Advances in Natural Science: Theory and Applications*, 4(2), 1-12.
- [38] Abrashev, B., Uzun, D., Kube, A., Wagner, N., & Petrov, K. (2020). Optimization of the bi-functional oxygen electrode (BOE) structure for application in a Zn-air accumulator. *Bulgarian Chemical Communications*, 52(2), 245–249. doi:10.34049/bcc.52.2.5100.
- [39] Nicheva, D., Abrashev, B., Piroeva, I., Boev, V., Petkova, T., Petkov, P., & Petrov, K. (2020). NiCo<sub>2</sub>O<sub>4</sub>/Ag as catalyst for bi-functional oxygen electrode. *Bulgarian Chemical Communications*, 52(Special Issue E), 68-72.
- [40] Abrashev, B., Uzun, D., Kube, A., Wagner, N., & Petrov, K. (2020). Optimization of the bi-functional oxygen electrode (BOE) structure for application in a Zn-air accumulator. *Bulgarian Chemical Communications*, 52(2), 245–249. doi:10.34049/bcc.52.2.5100.
- [41] Zinc-Air Secondary Innovative Nanotech Based Batteries for Efficient Energy Storage (ZAS), EU Horizon 2020 framework NMP Project GA 646186. Available online: <https://www.sintef.no/projectweb/zas> (accessed on April 2023).
- [42] Innovative Rechargeable (2023). National Science Fond of Bulgarian Ministry of Education and Sciences, Innovative rechargeable carbon-free zinc-air cells. INOVI, Project GA No. KP-06-H27-15/14.12.2018. Available online: <https://inovi.iees.bas.bg/> (accessed on April 2023).
- [43] Mladenova, E., Vladikova, D., Stoyanov, Z., Chesnaud, A., Thorel, A., & Krapchanska, M. (2013). Gases permeability study in dual membrane fuel cell. *Bulgarian Chemical Communications*, 45(3), 366–370.
- [44] Slavova, M., Mihaylova-Dimitrova, E., Mladenova, E., Abrashev, B., Burdin, B., & Vladikova, D. (2020). Zeolite based air electrodes for secondary batteries. *Emerging Science Journal*, 4(1), 18–24. doi:10.28991/esj-2020-01206.
- [45] Stoyanov, Z., Vladkova, D. (2005). *Differential Impedance Analysis*, Marin Drinov Academic Publishing House, Sofia, Bulgaria.
- [46] Tian, W. W., Ren, J. T., Lv, X. W., & Yuan, Z. Y. (2022). A “gas-breathing” integrated air diffusion electrode design with improved oxygen utilization efficiency for high-performance Zn-air batteries. *Chemical Engineering Journal*, 431. doi:10.1016/j.cej.2021.133210.